Beam-Based Alignment of the NLC Main Linac, Part One: Single-Bunch Comparative Study of Three Algorithms

Peter Tenenbaum
LCC-Note-0013
17-February-1999

Abstract

We describe the results of a series of simulation studies of beam-based alignment of the NLC main linacs using the program LIAR. Three algorithms for alignment of quadrupoles and girders are considered: the algorithm used in the ZDR, the ZDR algorithm combined with a post-alignment MICADO operation, and an algorithm which requires no steering dipoles but requires twice as many alignment segments per linac as the ZDR algorithm. The third algorithm appears to be the most robust, based on convergence time, required quad mover step sizes, and variation in extracted beam emittance as a function of BNS profile. We also study the effect of structure BPM resolution and ATL misalignments during the alignment process.

1 Introduction

Beam-based alignment and steering of the NLC main linac is expected to be an essential operation for control of emittance dilution due to wakefields and dispersion. The main linac design incorporates a vast amount of equipment (described below) for real-time alignment of the accelerator based on beam diagnostic signals.

The performance of the main linac depends not only upon the specifications of beam instrumentation and control devices, but also the algorithm which transforms data from the former into commands for the latter. The SLAC linac steering package contains a bewildering variety of algorithms (MICADO, one-to-one, RMS, SVD, 2BDFS), each of which represents certain trade-offs in speed, robustness, and payoff (in the form of a low-emittance beam and/or a maintainable orbit). In this Note we consider three possible algorithms for steering the main linac of the NLC based on beam-diagnostic data. The performance of each is assessed in terms of: convergence speed; residual emittance dilution; hardware performance required for convergence; and sensitivity to the linac phase configuration (ie, BNS phase profile). On the basis of these studies, an unusually strong case is made for one of the three algorithms. This algorithm is further studied, in order to assess its performance with different assumptions about RF Structure BPM ("S-BPM") resolution. A further study, in which ground motion induces misalignments of the accelerator during the alignment process, is also described.

2 Main Linac Design

The NLC main linac design used in this study is the CD-1 lattice of June, 1998. In this design the linac contains 4,962 X-Band (11.424 GHz) RF structures, each 1.8 meters long, resulting in an extracted beam energy of 500 GeV. The structures are installed on 6 meter girders, with 3 structures per girder. The linac also contains 724 quadrupoles, including a matching section from the second bunch compressor, three diagnostic regions, and three "supersectors" of interleaved RF girders and quadrupoles: the first, second, and third supersectors contain 1, 2, or 3 RF girders per quadrupole, respectively. Figure 1 shows the horizontal betatron function throughout the main linac. Note that the phase advance per cell is not uniform in the first 2 supersectors, but is tapered for optimal performance. The RF structures are modelled for wakefield purposes as RDDS-1 type, with an aperture $a/\lambda = 0.18$. The Green functions for the transverse and longitudinal wakefields (short-range) for this structure are in Figure 2.

The instrumentation and control devices in the design which are relevant to beam-based alignment and steering are:

- A beam position monitor ("Q-BPM") in the bore of each quad, with a pulse-to-pulse resolution of 1 μ RMS, and a static offset (BPM center-quad center) of 2 μ RMS

- A beam position monitor ("S-BPM") at the upstream end of each RF structure, and another at the downstream end of each structure, each with a pulse-to-pulse resolution of 5 μ RMS, and no static offset
- A remote-controlled precision magnet mover under each quad capable of moving the quad in x and y independently, with a sub-micron step size
- A remote-controlled precision girder mover at each end of each girder capable of moving in x and y with infinite precision
- Horizontal and vertical steering correctors at each quad location.

3 Beam Conditions

The beam conditions used for the study are based on the present "Option C" parameters: a bunch charge of 1.1×10^{10} and a bunch length of 145 μ. The normalized injection emittances were assumed to be 3.6×0.04 m.rad, which are somewhat larger than the assumed damping-ring extraction emittances. The injection energy and energy spread were 10 GeV and 1.5%, respectively. For the purposes of this study only a single bunch was used, rather than a bunch train. No jitter in position, angle, intensity, energy, energy spread, or injection timing were included in the study. No feedbacks were included in the study. It was assumed at all times that the beam energy is properly matched to the quadrupole strength at each quad, and that the incoming beam is also perfectly matched.

A total of 8 BNS profiles were used during the course of the study. These are the profiles which were used for ISG-2, and are summarized in Table 1. In each case the extracted energy spread is 0.3%.

BNS Case	Energy Overhead (%)	Phase 1 (deg)	Switch 1 (GeV)	Phase 2 (deg)	Switch 2 (GeV)	Phase 3 (deg)
1	1.3	4	30	-7	420	-30
2	1.9	8	30	-5	395	-30
3	2.5	10	30	-3	370	-30
4	3.1	12	30	-1	350	-30
5	3.7	14	30	1	325	-30
6	4.3	16	30	3	310	-30
7	4.9	18	30	5	295	-30
8	5.5	20	30	7	280	-30

Table 1: BNS Profiles used in this study. All profiles result in a final energy spread of 0.3%. Profiles courtesy G. Stupakov.

4 Simulation Software

All simulations used the program LIAR [1]. LIAR performs beam tracking with chromatic distortions from quadrupoles, and also convolves the beam with the longitudinal and transverse wakefields of the RF structure. LIAR Versions 2.1, 2.2, and 2.2.1 were used for the study.

While LIAR permits RF girders to be translated in x and y, pitched, and yawed, it does not include effects of pitching or yawing the structures themselves: a "pitched" girder has 3 un-pitched structures, each of which is at a different elevation, as shown in Figure 3. However the effect of a pitched or yawed girder is expected to be small [2].

All simulations were performed in the vertical plane, which is expected to be by far the most sensitive due to its smaller emittance. As an initial condition all quads were misaligned by 50 μ RMS, all girders were misaligned by 50 μ RMS, and all RF structures were misaligned by 15 μ RMS. Remote-controlled movers can compensate for quad or girder misalignments, but not structure misalignments.

5 Description of Algorithms

All of the steering algorithms share common requirements: they must reduce the emittance dilution due to wakefields and dispersion as much as possible, operate in a finite time, and prevent any corrective element from exceeding its maximum strength and/or excursion. All of the algorithms use the basic optical model of the accelerator for their calculations, and neglect wakefields. Because the algorithms neglect wakefields but the beam does not, it is necessary to iterate each algorithm, and also to divide the accelerator into short sections over which the optical beam transport is more significant than the wakefield effects.

Beyond these commonalities, the algorithms have considerable differences. Each one is described in detail below.

5.1 Canonical Algorithm

This is the algorithm which was used for ZDR studies of the main linac. The linac is divided into N subsections, each containing approximately an equal number of quads. In each section the following series of steps is followed:

- Read out all the Q-BPMs on a single pulse
- Using the optical transport matrices, compute the set of magnet moves which will simultaneously minimize the RMS of the BPM readings and the RMS movements of the magnets
- Apply the quad moves computed
- Read out all the S-BPMs on a single pulse
- Move each girder's endpoints to zero the average of the S-BPMs on that girder
- Iterate above steps m times; note that region $n-1$ is aligned m times before region n is aligned at all

In order to simultaneously minimize the magnet moves and the BPM readings, it is useful to apply different weights to the two contributions. In all cases the BPM readings were given a weighting factor of 4 μ, while quad moves were given a weighting factor of 1000 μ. This means that a BPM reading of 4 μ would increase χ^2 by 1, while a magnet move of 1000 μ would produce the same increase in the χ^2.

An additional refinement of the algorithm is that the first quad of region n is also the last quad in region $n-1$. Furthermore, the algorithm uses a corrector at the first quad in a region to steer the beam into the center of the last quad. Therefore, the first and last quad in any region do not get moved. The algorithm basically picks a series of segment endpoints, smooths the alignment of quads and girders between the endpoints, and uses a set of correctors to steer from one endpoint to another, as shown in Figure 4.

For all simulations described in this note, N was set to 14 segments, each of which contains approximately 50 quads.

5.2 MICADO "Afterburner"

In the case of coarse magnet mover step sizes, it was often found that the Canonical algorithm produced an orbit with a non-zero betatron component. This is due to poorly-aligned magnets at the same betatron phase combining to produce a large oscillation.

One of the standard techniques to address betatron oscillations is the MICADO algorithm [3]. The MICADO algorithm was added to the Canonical algorithm as follows:

- Perform Canonical algorithm on segment n, for m iterations
- Read all the Q-BPMs on a single pulse
- Using the optical transport matrices, identify the single quad which, when moved, minimizes the RMS orbit through the segment; latch that quad
- Repeat the 2 steps above, identifying the single quad which, when used with the latched first quad, minimizes the RMS orbit through the segment.

- Iterate the steps above, "latching" an additional quad on each iteration, until the maximum number of quads are latched, or the RMS orbit falls below a given threshold
- Apply moves to "latched" quads
- Perform RF girder alignment as described above
- Iterate entire MICADO procedure on segment n for p iterations total.

The combination of Canonical and MICADO algorithms is clearly more time-consuming than the Canonical alone, since *both* algorithms need to be iterated several times to converge. For the purposes of this study the maximum number of magnets to be moved by MICADO in a segment was fixed at 7, and the desired RMS orbit tolerance was set to 1 μ.

5.3 "French Curve"

The Canonical algorithm assumes that horizontal and vertical correctors are available at each quad, and that any quad can be used as a segment endpoint. At present it is assumed that steering correctors will be placed at only a few locations, and those will be used primarily by steering feedback. The "French Curve" algorithm is a steering algorithm similar to the Canonical, but one which does not require corrector magnets. The algorithm proceeds as follows:

- Perform alignment of segment n as in the Canonical algorithm, but do not use a corrector at the first quad to steer to the last quad; iterate m times
- Select a segment starting at the *center* quad of segment n and ending at the *center* quad of segment $n+1$; perform the alignment of this segment, iterating m times
- Move to segment $n+1$, etc.

By aligning in full segments, but advancing down the linac in half-segments, the magnet and girder positions follow the approximate mechanical survey line without the use of correctors to kink the beam at segment boundaries.

For all simulations described in this Note, a total of 27 segments were selected, each of which contained approximately 50 quads.

6 Results of Simulations

Each simulation of each algorithm was performed with 100 seeds, and the average and standard deviation of the mean (RMS/$\sqrt{100}$) was recorded. These are plotted as a function of the independent variable for studies below.

6.1 Convergence Speed

Figure 5 shows the residual emittance dilution of the Canonical and French Curve algorithms as a function of iterations/segment. BNS profile 5 (3.7% overhead) and mover step size of 50 nm were used. Note that while the Canonical algorithm requires 5 iterations/segment to converge, the French Curve alignment uses almost twice as many segments as the Canonical. Thus, the Canonical will converge in slightly less time.

6.2 Magnet Mover Step Size

Figure 6 shows the increase in normalized emittance after each of the algorithms described above. In all cases BNS Profile 5 was used. The Canonical algorithm used 5 iterations/segment, the Canonical+MICADO used 5 iterations/segment of the former and 3 of the latter, while the French Curve algorithm used 3 iterations/segment. While all the algorithms degrade somewhat in performance for step sizes approaching 0.3 μ, the Canonical algorithm deteriorates much more quickly than the other two. While use of MICADO

can recover most of this additional dilution, it cannot improve to the level of the French Curve algorithm. This appears to be a function of the dispersion introduced by the Canonical algorithm's correctors.

We conclude from Figure 6 that if the magnet movers are unable to achieve 50 nm step sizes (which is the present design), good control of the emittance will still be possible.

6.3 BNS Profile

Figure 7 shows the residual emittance dilution for the BNS profiles in Table 1, for Canonical and French Curve algorithms. In all cases the mover step size was 50 nm, and each of the algorithms was permitted to iterate to convergence (5 and 3 iterations/segment, respectively). In all cases the Canonical algorithm results in higher emittances than the French Curve algorithm, which is expected from Figure 6. What is not intuitive is that more BNS overhead results in *larger* emittances after alignment! This is counter to the usual "more is better" logic of BNS phasing, and also to studies of jitter and single-element misalignments [4].

This can be explained by the fact that BNS damping primarily stabilizes the beam against betatron oscillations, by causing the wakefield-deflection and the dispesive deflection at a given location to cancel one another. This can only be the case if the beam's offset from the center of the accelerator is large compared to the short-range misalignments of the accelerator components. Because this study does not include jitter, the beam offset and the short-range misalignments are both on the order of a few microns, and therefore dispersive and wake kicks do not cancel in this case. It will be necessary to pick a BNS profile which provides sufficient stability against betatron oscillations and other coherent phenomena while not spoiling the "on-axis" beam unacceptably.

7 Additional Simulations

On the basis of the results above, the French Curve algorithm seems clearly better than the alternatives. We performed two additional simulations using just the French Curve algorithm.

7.1 S-BPM Resolution

Figure 8 shows the residual emittance dilution as a function of the resolution of the S-BPMs. While resolutions up to 10 μ are acceptable, poorer resolutions quickly degrade the emittance at the end of the linac.

7.2 Ground Motion

In recent years Shiltsev has proposed a diffusive model for ground motion, in which the mean-squared transverse distance between two elements is proportional to the longitudinal distance between them and the time elapsed (assuming a perfect alignment at $t = 0$) [5]. This is usually referred to as the "ATL Law:" $\sigma^2_{x,y} = A \cdot t \cdot L$. The value of A is a function of local cultural noise, ground conditions, and other variables, and can range over several orders of magnitude; however, at a *given* site, with fixed conditions, the value of A can be stable over several years.

The ATL law means that while the operators are aligning the accelerator, natural processes are simultaneously misaligning it. We studied this interaction by assuming a value for A and an average time t per action (where one action is one iteration of quadrupole or structure misalignment). We assumed that all quad or structure movers in a segment moved simultaneously and not consecutively.

The value of A ranges from 10^{-4} to 10^{-8} μ^2/(meter.second). The ZDR assumes that, through a combination of site selection and engineering, the NLC value of A can be held to 5×10^{-7} in these units, which is low but not unachievable. We use this value in these studies.

For the time to complete one operation we assumed the following: the initial alignment of the accelerator, from the severely-misaligned initial conditions to convergence, would utilize 3 iterations/segment; each iteration would consist of 1 pass of quad alignment, and one pass of girder alignment; each pass of quad or girder alignment would require 60 seconds to complete. Thus each segment takes 6 minutes for 3 iterations, and the total time for the linac alignment is 3 hours. Once the initial alignment is complete, we assumed

that the alignment procedure would continue, aligning from the upstream to the downstream; however, this stage of the alignment would use 1 iteration/segment, and 30 seconds per operation. The rationale for this is that the major alignment would be overseen by humans because large moves are made, thus taking more time, while the continuing alignment is only responding to small perturbations from the ATL processes, and therefore it can function with fewer iterations and can be automated (requiring less time).

Figure 9 shows the results of alignment with ATL processes: iteration 0 is the human-supervised, long-and-slow alignment, while iterations 1 through 3 are automated, short-and-fast operations. The equilibrium emittance dilution is increased from 34% to 49% by ground motion.

8 Conclusions

We have reported on simulation studies of 3 alignment/steering algorithms for the NLC main linac. Of the three, the French Curve algorithm is the clear favorite due to its low residual emittance, relaxed hardware requirements, low sensitivity to BNS profile, and acceptable convergence time.

The French Curve algorithm requires S-BPM resolution on the order of 5 μ in order to achieve best results; poorer resolutions rapidly degrade the emittance. While the algorithm is sensitive to ATL-like ground motion disturbances, by automating the algorithm the ATL dilutions can be held to acceptable limits.

9 Further Study

This Note only scratches the surface of alignment issues in the NLC main linac. Some additional effects which must be studied are:

- Second-order effects: how does alignment coupled with various other errors (phase, voltage, quad strength, bunch length, bunch timing, quad roll) change the resulting emittance dilution and/or sensitivity to jitter?
- Feedbacks: can a few feedbacks improve the performance under ATL conditions?
- S-BPMs: the model above unrealistically assumes that S-BPMs have no static offsets. If the RF structure is bowed, for example, then BPMs at the upstream and downstream ends will have a static offset from the electrical center of the structure. This needs to be studied.
- Multibunch effects: we have ignored any multibunch phenomena in this study. Long range wakefields, bunch-to-bunch energy errors, and odd response of S-BPMs to a non-straight bunch train are all issues which require further study.

10 Acknowledgements

The assistance and encouragement of R. Assmann, T. Raubenheimer, G. Stupakov were indispensible in the production of this Note.

References

[1] R. Assmann *et al.* "LIAR: A New Program for the Modeling and Simulation of Linear Accelerators with High Gradients and Small Emittances," SLAC-PUB-7300. In *Proceedings of the 18th International Linac Conference* (1996), pg 464.

[2] G. Stupakov, private communication.

[3] B. Autin and Y. Marti. "Closed Orbit Correction of A.G. Machines Using a Small Number of Magnets." CERN ISR-MA/73-17 (1973).

[4] G. Stupakov. "BNS Profiles and Sensitivity of Beam Orbit of the NLC Linac." LCC-Note-0012 (1999).

[5] V. Shiltsev. “Space-Time Ground Diffusion: The ATL Law for Accelerators.” In *Proceedings of the Fourth International Workshop on Accelerator Alignment* (1996), pg. 352.

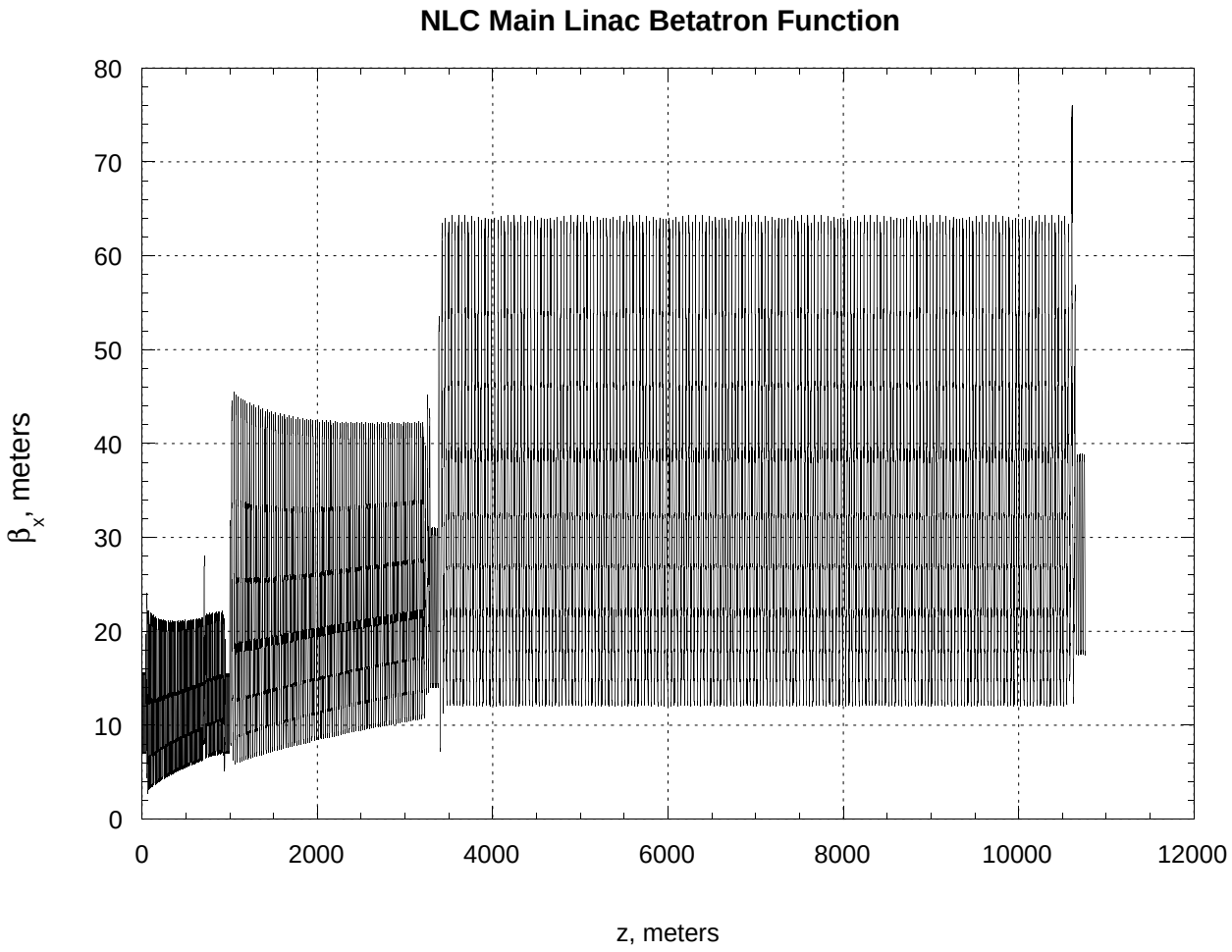

Figure 1: Horizontal betatron function in NLC main linac, June 1998 design.

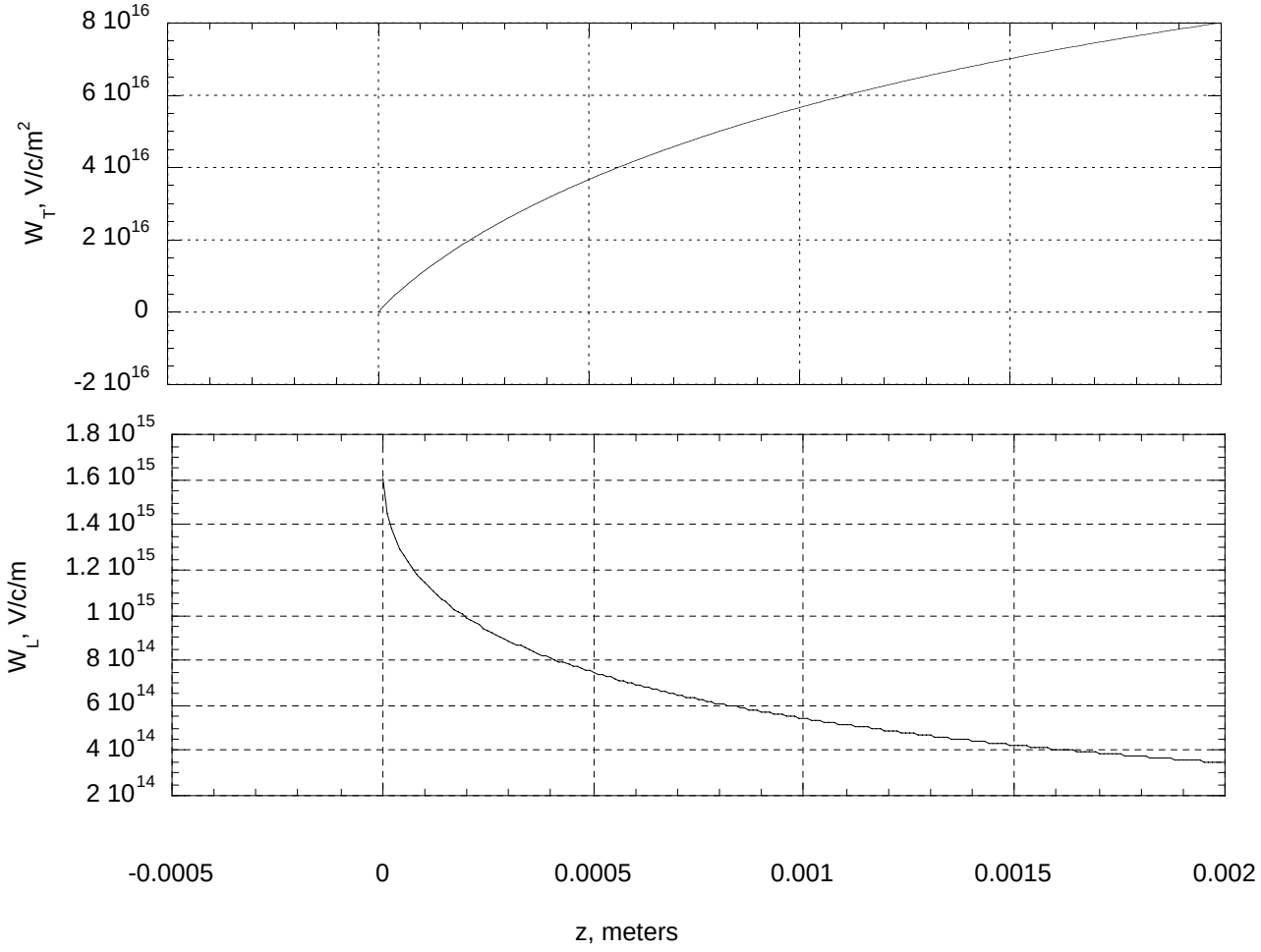

Figure 2: Short-range wakefield Greens function for RDDS-1: transverse wake (top) in V/c/m^2, longitudinal wake (bottom) in V/c/m.

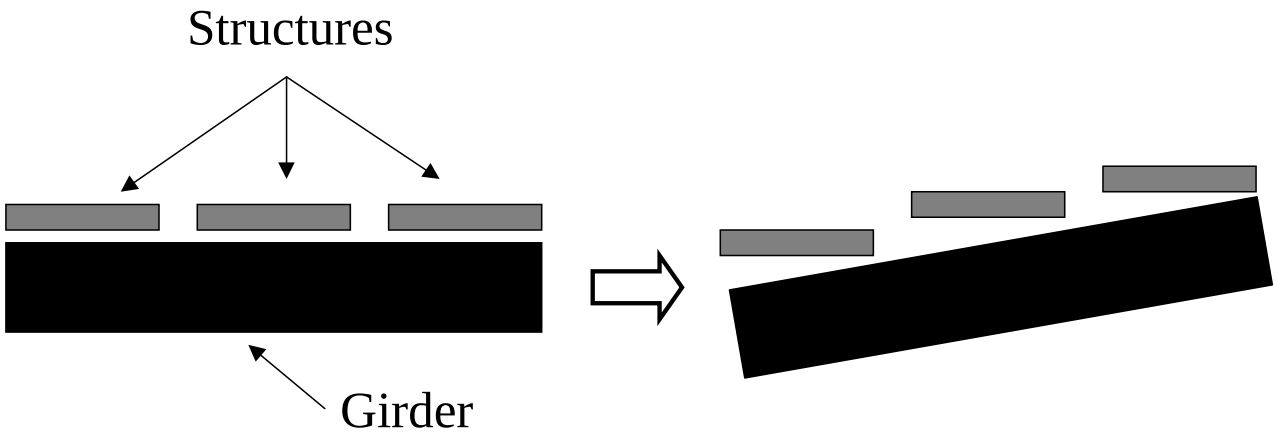

Figure 3: How LIAR simulates pitching of an RF structure girder. The structures are translated proportionally to their disances from either endpoint, but the structures are not themselves pitched in the simulation.

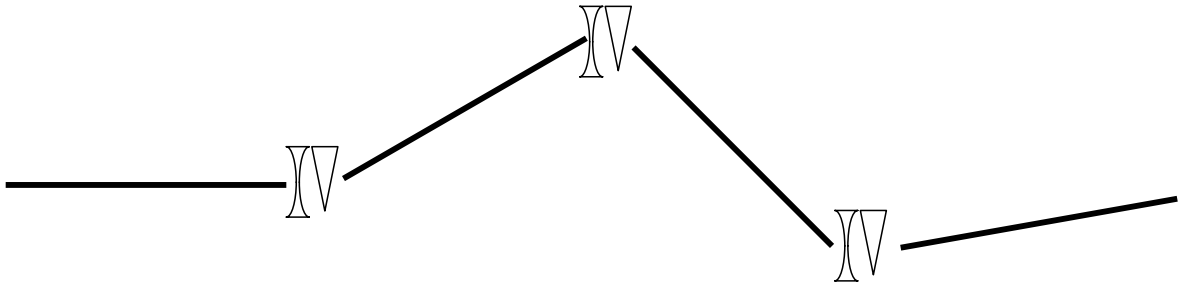

Figure 4: Diagram of Canonical alignment algorithm. A number of quads are selected as fixed endpoints to linac segments. The quads and structures between endpoints are moved to the straight line between endpoints, and correctors at each endpoint steer the beam into the next segment.

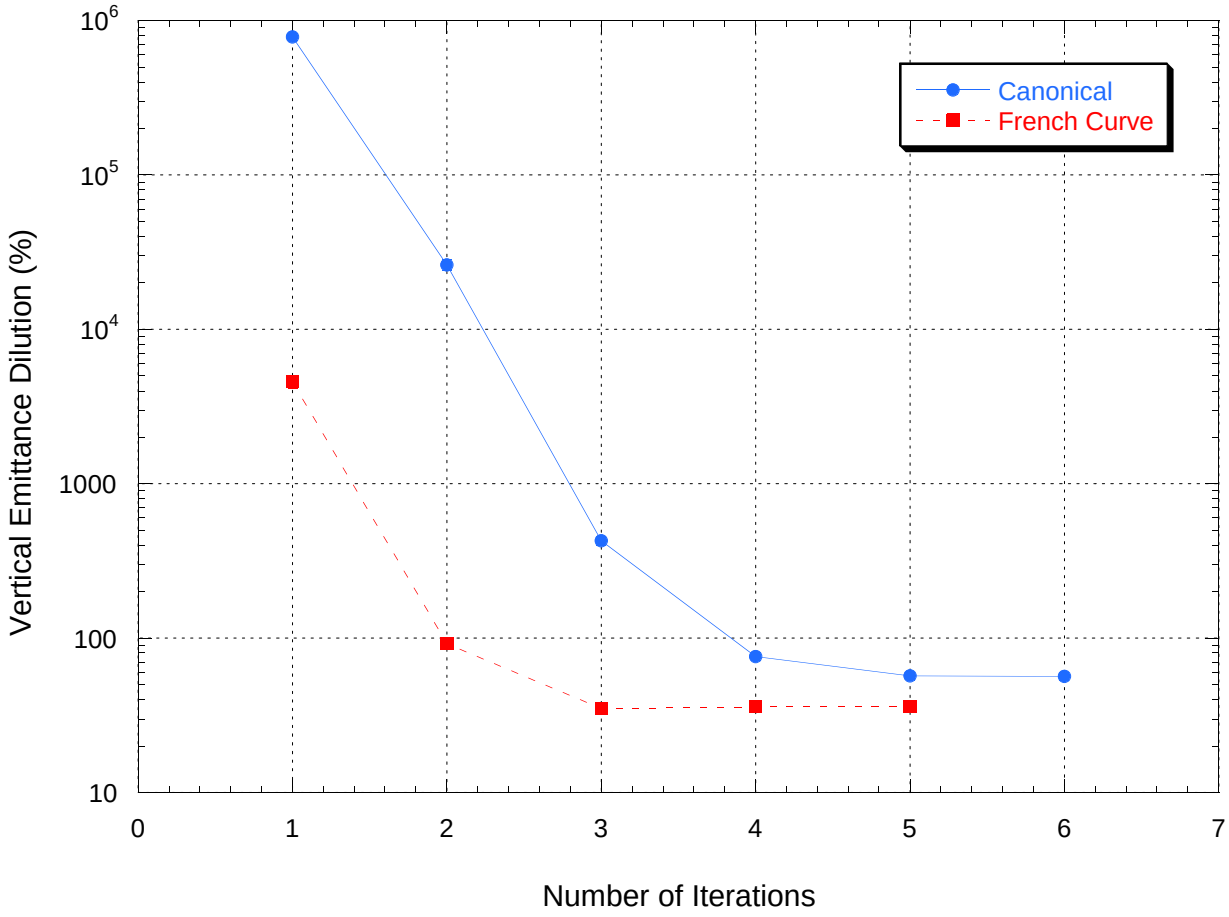

Figure 5: Number of iterations/segment required for convergence of the Canonical and French Curve algorithms.

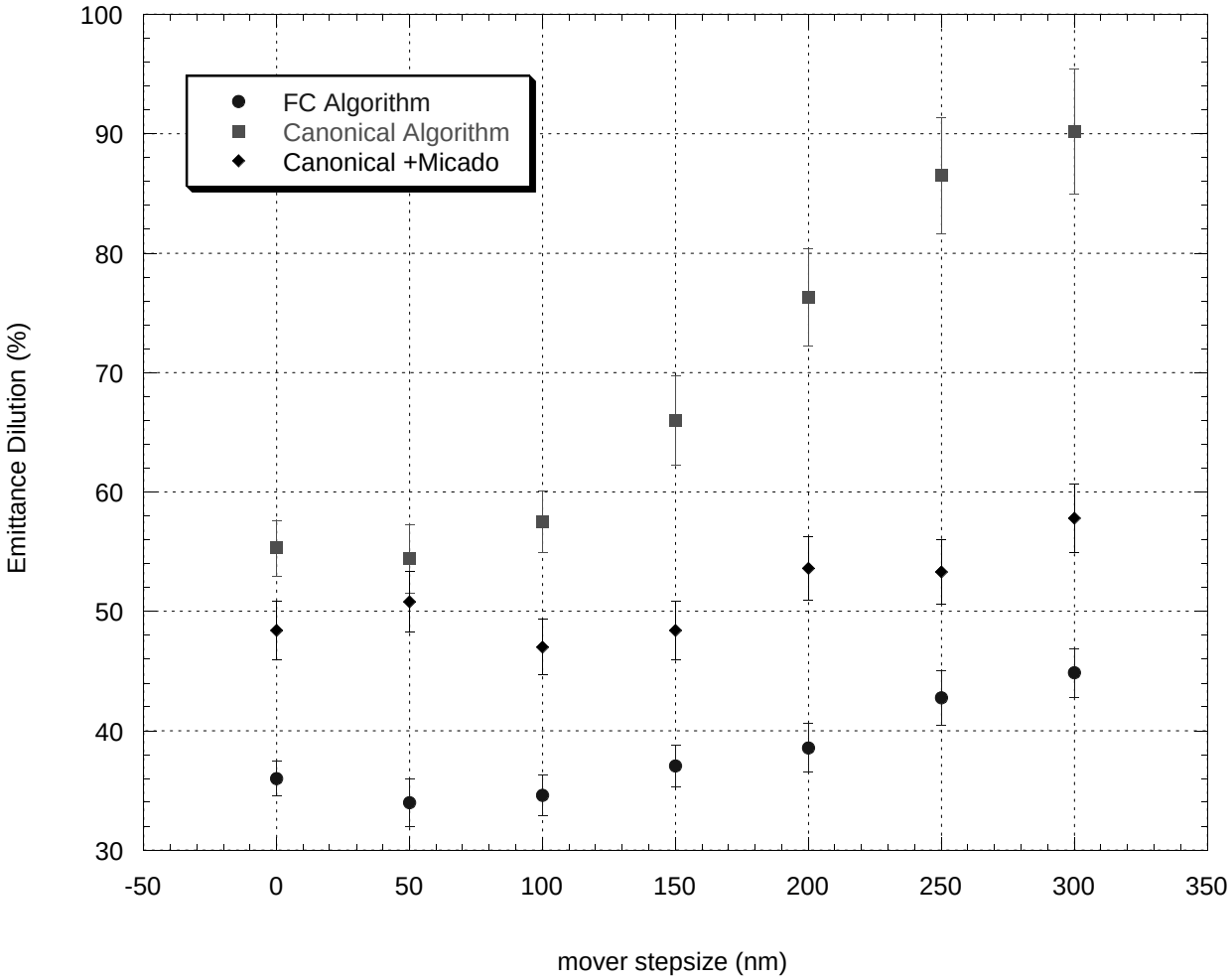

Figure 6: Residual emittance dilution as a function of stepsize for Canonical, Canonical+MICADO, and French Curve alignment algorithms.

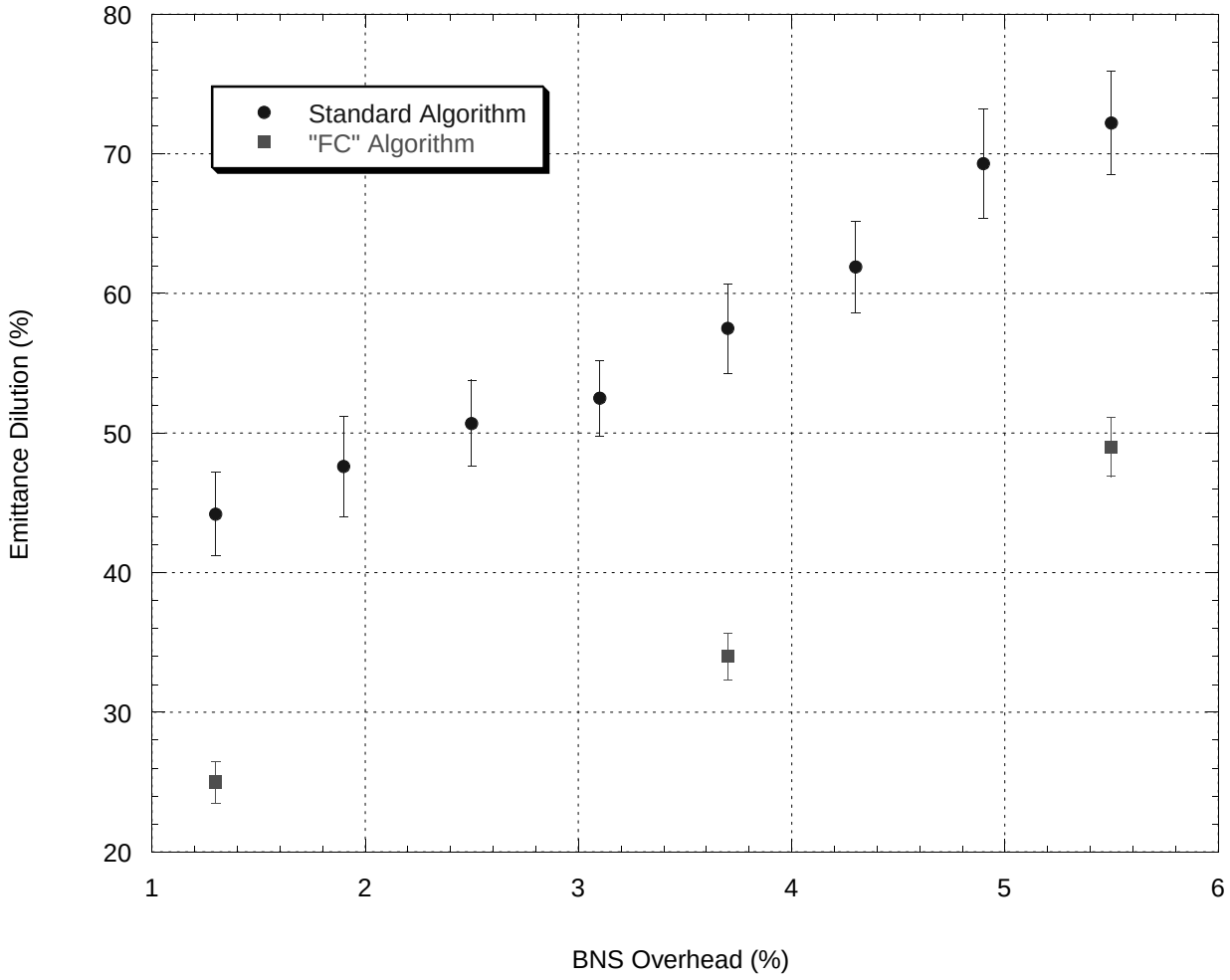

Figure 7: Residual emittance dilution as a function of BNS overhead for Canonical and French Curve alignment algorithms.

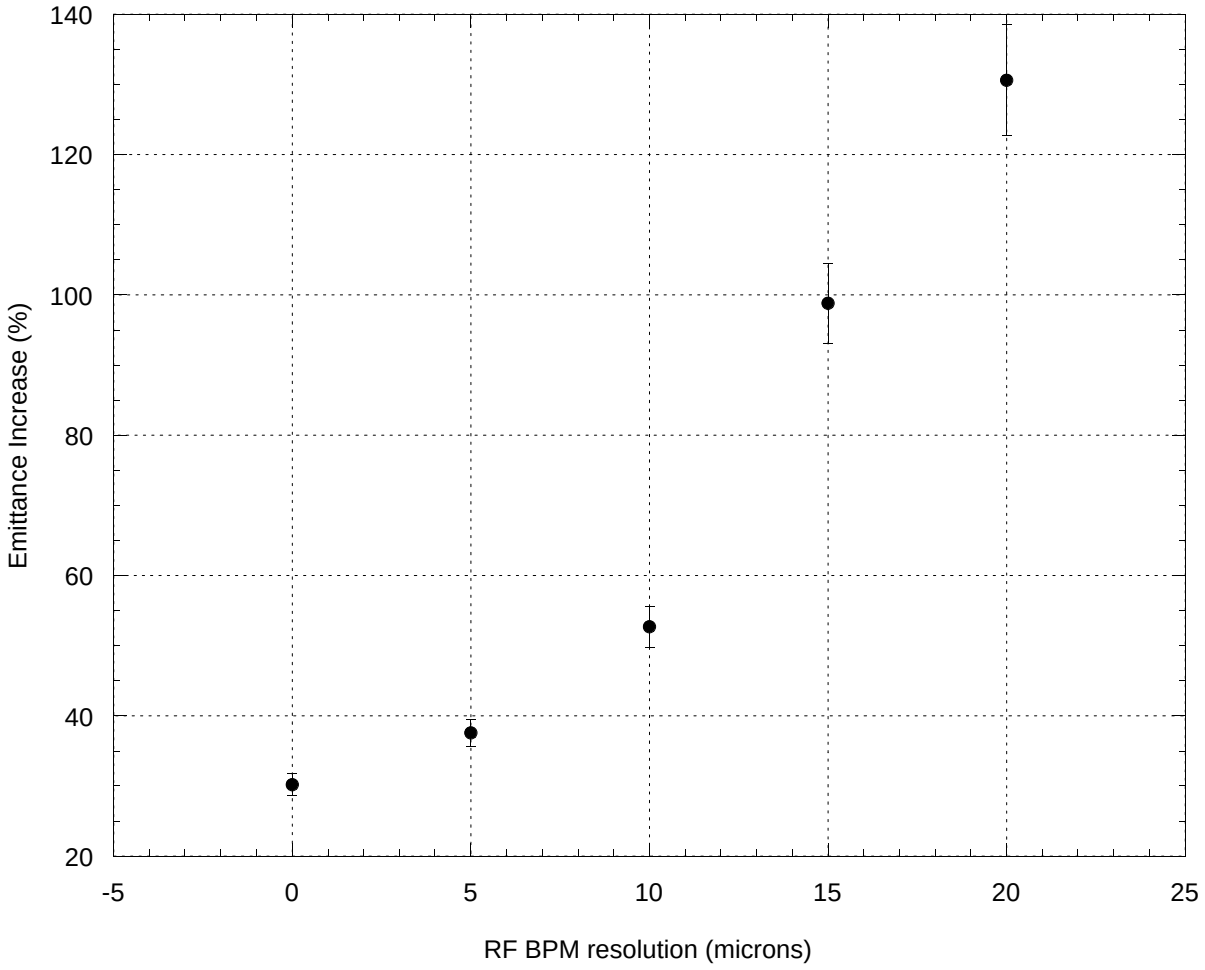

Figure 8: Emittance dilution as a function of S-BPM resolution.

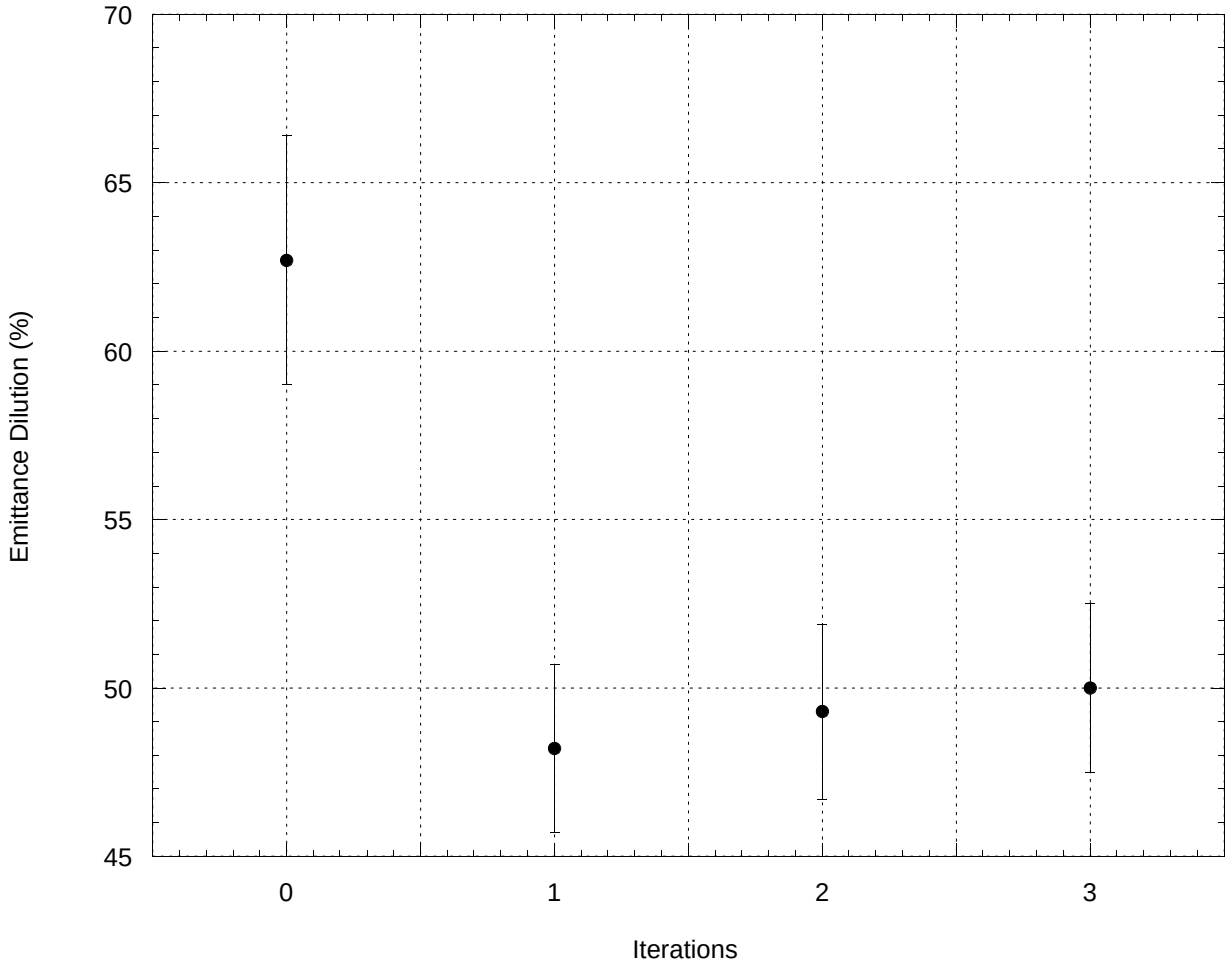

Figure 9: Emittance dilution due to ATL misalignments during alignment process. Iteration 0 is a large, time-consuming alignment which requires 3 hours for the full linac, while iterations 1 through 3 require only 30 minutes per linac. An ATL coefficient of $5 \times 10^{-7} \mu^2/\mathrm{m/sec}$ is assumed.